

Nanostructured Thermosetting Blends of Epoxy Resin and Amphiphilic Poly(ϵ -caprolactone)-*block*-polybutadiene-*block*-poly(ϵ -caprolactone) Triblock Copolymer

Fanliang Meng,[†] Sixun Zheng,^{*,†} Weian Zhang,[†] Huiqin Li,[‡] and Qi Liang[‡]

Department of Polymer Science and Engineering, Instrumental Analysis Center, Shanghai Jiao Tong University, 800 Dongchuan Road, Shanghai 200240, P. R. China

Received August 23, 2005; Revised Manuscript Received November 21, 2005

ABSTRACT: The amphiphilic triblock copolymer poly(ϵ -caprolactone)-*b*-polybutadiene-*b*-poly(ϵ -caprolactone) (PCL–PB–PCL) was synthesized via the ring-opening polymerization of ϵ -caprolactone in the presence of a hydroxyl-terminated polybutadiene (HTPB), which was catalyzed by stannous octanoate [Sn(Oct)₂]. The amphiphilic triblock copolymer was further used to prepare the nanostructured epoxy thermosets. The in situ polymerization of epoxy monomers in the presence of PCL–PB–PCL started from the homogeneous solutions composed of the block copolymer and the monomers of epoxy at the temperature above the upper critical solution temperature (UCST) of diglycidyl ether of bisphenol A (DGEBA) and HTPB blends. The transmission electronic microscopy (TEM), small-angle X-ray scattering (SAXS), and atomic force microscopy (AFM) showed that the nanostructured thermosets were successfully obtained. Depending on the content of the block copolymer in the thermosets, the PB domains can display spherical and interconnected nanoobjects with the size of 10–20 nm. It is judged that the nanostructures are formed on the basis of the mechanism of polymerization-induced microphase separation, which is in a marked contrast to the approach in which some equilibrium self-organized structures were preformed and the microphases were fixed via subsequent curing reaction.

Introduction

Over the past decades, considerable progress has been made to understand the relationship between morphological structures and resulting properties of multicomponent thermosetting blends.¹ This progress is, in part, a consequence of the recognition of the importance of toughening mechanisms in rubber (or thermoplastics)-modified epoxy resins. Most of the thermosetting blends are prepared starting from a homogeneous solution of thermoplastic (or rubbery) polymers in thermoset precursors. Since these modifiers are some linear homopolymers or random copolymers, so-called reaction-induced phase separation generally occurs on the macroscopic scale with the polymerization proceeding.¹ The phase behavior of thermosetting blends is quite dependent on several competitive kinetics (and/or dynamics) such as curing reactions and phase separation in the composite systems. Thermodynamically, the driving force for reaction-induced phase separation is the unfavorable entropic contribution (ΔS_m) to the mixing free energy resulting from the dramatic increase in molecular weight owing to polymerization. Nonetheless, the miscible thermosetting blends can be accessed when there exist the favorable intermolecular specific interactions (e.g., hydrogen bonding), which affords the exothermic mixing (i.e., $\Delta H_m < 0$).²

Recently, it is recognized that the formation of ordered (or disordered) nanostructure in thermosets could further optimize the interactions between thermoset matrix and modifiers and thus endow materials with improved properties.^{3,4} Bates et al.³ have precedently proposed a strategy of creating nanostructures using amphiphilic block copolymers. In this protocol, the

precursors of thermosets act as the selective solvents of block copolymers, and some self-assembly microphases such as lamellar, bicontinuous, cylindrical, and spherical structures are formed in the mixtures, depending on the blend composition before curing reaction. These nanostructures were further fixed with introduction of hardeners and subsequent curing. In this approach, some equilibrium self-organized structures were formed. With an appropriate design of block copolymer architecture, the block copolymers self-assemble to form ordered or disordered phases, and the role of curing is to lock in the morphology that is already present. In view of the strategy based on cross-linking with the self-organized phases, a variety of nanostructured thermosets have been designed and prepared.⁴

The premise for this approach is that the self-organized microphases are formed prior to curing in the composite systems. Nonetheless, this is not always achievable. In many cases, all the subchains of block copolymers are miscible with the precursors of thermosets due to the negligible entropic contribution (ΔS_m) to free energy of mixing (ΔG_m) since the molecular weights of the blend systems are quite low. In addition, the presence of self-organized microphases at lower temperatures does not purport that such nanoscopic structures can be survived at elevated temperatures that are required for curing of high-performance thermosets since the blends of polymers and low molecular weight compounds generally exhibit the upper critical solution temperature (UCST) behaviors.^{1,5} Under this circumstance, it is proposed that the nanostructures in thermosets should alternatively be able to form via the mechanism of reaction-induced microphase separation; i.e., the nanostructures can also be obtained by selectively controlling the microphase separation of certain subchains of block copolymers induced by polymerization whereas the other subchains remain miscible with the cross-linked thermosets. It is expected that in this case several variables such as kinetics of curing reaction and microphase

[†] Department of Polymer Science and Engineering.

[‡] Instrumental Analysis Center.

* To whom correspondence should be addressed: E-mail szheng@sjtu.edu.cn; Tel 86-21-54743278; Fax 86-21-54741297.

separation, composition of block copolymers, and the mixture of the precursors of thermosets and block copolymers can alternatively be employed to control the formation of nanostructures. However, this approach remains largely unexplored vis-à-vis the self-organization technique although the mechanism could actually be involved with the preparation of some nanostructured thermosets.⁶

The purpose of this work is to show that it is not necessary to preform the self-organized structure in the mixtures of diglycidyl ether of bisphenol A (DGEBA) and an amphiphilic triblock copolymer to prepare the nanostructured (ordered or disordered) thermosets. For this purpose, we design to synthesize an amphiphilic triblock copolymer, poly(ϵ -caprolactone)-*block*-polybutadiene-*block*-poly(ϵ -caprolactone), PCL-PB-PCL, knowing that (i) PCL is miscible with epoxy monomers before curing and also miscible with 4,4'-methylenebis(2-chloroaniline) (MOCA)-cured epoxy thermosets⁷ and (ii) the blend system composed of low molecular weight PB and epoxy precursors displayed an upper critical solution temperature (UCST) behavior and reaction-induced phase separation occurs when the blends are cured at elevated temperatures. Therefore, in the thermosetting blends of epoxy resin with PCL-PB-PCL the curing reaction can be initiated from a homogeneous solution at the temperature above the UCST of the system. It is expected that with the curing reaction proceeding we can selectively control the microphase separation of PB subchains induced by polymerization whereas the PCL subchains remain miscible with the cross-linked epoxy networks. As a consequence, the nanostructured epoxy thermosets can be prepared via so-called reaction-induced microphase separation. The phase behavior, intermolecular specific interactions, and nanostructures were investigated by means of phase-contrast microscopy (PCM), scanning electronic microscopy (SEM), Fourier transform infrared spectroscopy (FTIR), differential scanning calorimetry (DSC), transmission electron microscopy (TEM), small-angle X-ray scattering (SAXS), and atomic force microscopy (AFM). Finally, we address the mechanism responsible for the formation of nanostructures in the thermosets.

Experimental Section

Materials. Diglycidyl ether of bisphenol A (DGEBA) with epoxide equivalent weight of 185–210 was purchased from Shanghai Resin Co., China. The curing agent is 4,4'-methylenebis(2-chloroaniline) (MOCA), supplied by Shanghai Reagent Co., China. The monomer, ϵ -caprolactone (CL), was purchased from Fluka Co., Germany, and it was distilled over calcium hydride (CaH₂) in the decreased pressure prior to polymerization. Stannous octanoate [Sn(Oct)₂] was of analytical grade, purchased from Aldrich Co., and used as received. The hydroxyl-terminated polybutadiene (HTPB) was kindly supplied by Qilong Chemical Corp., Shandong province, China, and it was prepared via anionic polymerization. The HTPB has 20 mol % 1,2-addition and 80 mol % 1,4-addition structural units in which the content of *trans*-1,4 additional moieties is 60 mol %. It has a quoted molecular weight of $M_n = 3500$. Before use, the HTPB was dried by an azeotropic distillation using anhydrous toluene.

Synthesis of Triblock Copolymer. The synthesis of block copolymer was carried out using a standard Schlenk line system. The amphiphilic triblock copolymer, poly(ϵ -caprolactone)-*block*-polybutadiene-*block*-poly(ϵ -caprolactone) (PCL-PB-PCL) was synthesized via the ring-opening polymerization of ϵ -CL in the presence of hydroxyl-terminated polybutadiene (HTPB), and stannous octanoate [Sn(Oct)₂] was used as the catalyst. Prior to polymerization, all the glassware was carefully dried at 150 °C for 3 h and then in vacuo to ensure a waterless system. Typically, a round-bottom flask with 3.1 g (1.80 mmol of hydroxyls) of HTPB and a dry magnetic stirring bar was sealed. Then, 10.2 g (89.50

mmol) of ϵ -CL and Sn(Oct)₂ in anhydrous toluene was added to system. Toluene was removed under decreased pressure, and the amount of Sn(Oct)₂ was controlled as 1/1000 (wt) with respect to the total weight of the reactants. The polymerization was carried out at 110 °C for 48 h. The crude product was dissolved in dichloromethane and poured dropwise into an excess of diethyl ether, and this procedure was repeated three times to purify the samples. The resulting polymer was dried in a vacuum oven at 40 °C for 48 h prior to use. The polymer (13.034 g) was obtained with the yield (or conversion) of >98%. The molecular weight of the block copolymer was determined by means of ¹H NMR to be $M_n = 14\,600$. Fourier transform infrared spectroscopy (FTIR) (KBr window, cm⁻¹): 2943 (C–H, methylene of PCL), 1726 (C=O, ester of PCL); 967 (C–H, *trans*-1,4 of PB), 730 (C–H, *cis*-1,4 moieties of PB), 911 (C–H, 1,2-structure of PB). ¹H nuclear magnetic resonance spectroscopy (NMR) (chloroform-*d*, ppm): 4.04–4.07 [OCO(CH₂)₄CH₂, 4H], 2.28–2.32 [OCOCH₂(CH₂)₄, 4H], 1.60–1.68 [OCOCH₂CH₂CH₂CH₂CH₂, 8H], 1.35–1.41 [OCOCH₂CH₂CH₂CH₂CH₂, 4H], 5.26–5.50 [H₂CCH=CHCH₂ in 1,4 structure of PB, 1.6H], 2.04–2.12 [CH₂CH=CHCH₂ in 1,4 structure of PB, 3.2H], 4.85–5.04 [(CH₂)CH(CH₂)CH=CH₂ in 1,2 structure of PB, 0.6H], 1.83–2.16 [(CH₂=CH)CHCH₂ in 1,2 structure of PB, 0.2H], 1.19–1.34 [(CH₂=CH)CHCH₂ in 1,2 structure of PB, 0.4H].

Preparation of HTPB/DGEBA Blends. The HTPB/DGEBA blends were prepared by solution casting from tetrahydrofuran (THF) at room temperature. The concentration was controlled within 5% (w/v). To remove the residual solvent, all the blend films were further desiccated in vacuo at 50 °C for 48 h.

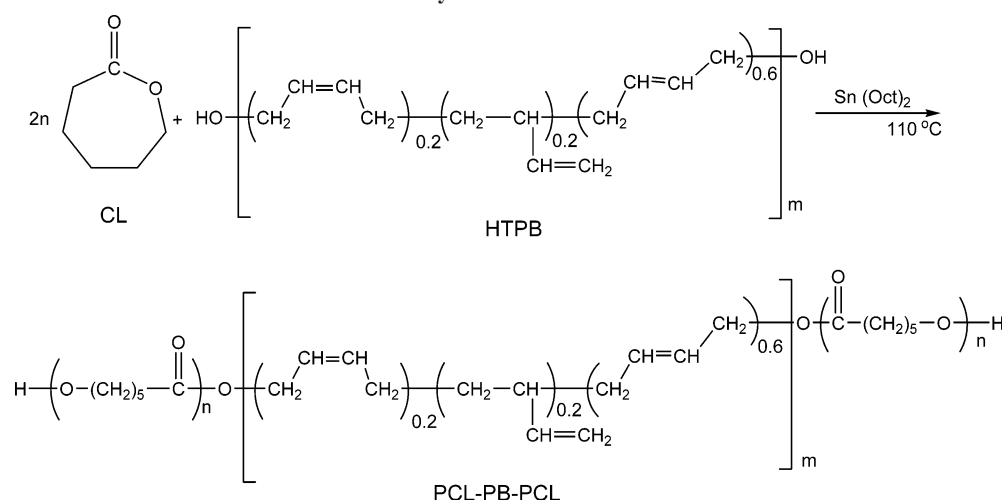
Preparation of Nanostructured Thermosets. The triblock copolymer PCL-PB-PCL was first dissolved with tetrahydrofuran (THF) (20 wt %), and then the solution was added to DGEBA at ambient temperature. The curing agent MOCA was added to system with vigorous stirring until homogeneous solutions were obtained. The mixtures obtained were heated to 60 °C with continuous stirring to remove the majority of THF and degassed in vacuo at 60 °C for 30 min to remove residual solvent. The ternary mixture was poured into Teflon molds and cured at 150 °C for 2 h plus 180 °C for 2 h for postcuring. The thermosets containing the block copolymer up to 50 wt % were obtained.

Measurement and Characterization. *Fourier Transform Infrared Spectroscopy (FTIR).* The FTIR measurements were conducted on a Perkin-Elmer Paragon 1000 Fourier transform spectrometer at room temperature (25 °C). The block copolymer was dissolved with THF (10 wt %), and the solution was cast onto a KBr windows. The solvent was eliminated in a vacuum oven at 60 °C for 30 min. The specimens of thermosets were granulated, and the powder was mixed with KBr pellets to press into the small flakes for measurements. All the specimens were sufficiently thin to be within a range where the Beer–Lambert law is obeyed. In all cases 64 scans at a resolution of 2 cm⁻¹ were used to record the spectra.

Nuclear Magnetic Resonance Spectroscopy (NMR). The NMR measurements were carried out on a Varian Mercury Plus 400 MHz NMR spectrometer at 25 °C. The samples were dissolved with deuterated chloroform, and the solutions were measured with tetramethylsilane (TMS) as the internal reference.

Phase Contrast Microscopy (PCM). A Leica DMLP polarized optical microscope equipped with a hot stage (Linkam TH960, Linkam Scientific Instruments, Ltd., UK) with a precision of ± 0.1 °C was used for the determination of the cloud point curve of DGEBA/HTPB mixtures. The THF solutions of the mixtures were cast onto cover glasses; the majority of solvent was removed at 50 °C, and the residual solvent was further eliminated by drying the samples in vacuo at 50 °C for 2 h. The films of the blends were sandwiched between two cover glasses. For measurements of the cloud point curve (CPC), the blend films with various compositions were observed under a polarizing microscope in which the angle between the polarizer and analyzer was 45°. The samples were heated through the cloud points at a rate of 5 °C/min, and the cloud

Scheme 1. Synthesis of PCL-PB-PCL



point was defined as the onset of the turbidity. The cloud points were plotted as a function of blend composition.

Differential Scanning Calorimetry (DSC). The calorimetric measurements were performed on a Perkin-Elmer Pyris 1 differential scanning calorimeter in a dry nitrogen atmosphere. An indium standard was used for temperature and enthalpy calibrations. The samples (about 8.0 mg in weight) were first heated to 180 °C and held at this temperature for 3 min to remove the thermal history, followed by quenching to -60 °C. A heating rate of 20 °C/min was used at all cases. The glass transition temperature (T_g) was taken as the midpoint of the heat capacity change. The crystallization temperatures (T_c) and the melting temperatures (T_m) were taken as the temperatures of the minimum and the maximum of both endothermic and exothermic peaks, respectively.

Small-Angle X-ray Scattering (SAXS). The SAXS measurements were taken on a Bruker AXS D8 Discover GADDS system. Two-dimensional diffraction patterns were recorded using an image intensified CCD detector. The experiments were carried out at room temperature (25 °C) or elevated temperature using Cu K radiation ($\lambda = 1.54$ Å, wavelength) operating at 40 kV, 35 mA. The intensity profiles were output as the plot of scattering intensity (I) vs scattering vector, $q = (4\pi/\lambda) \sin(\theta/2)$ (θ is the scattering angle).

Scanning Electron Microscopy (SEM). To observe the phase structure of epoxy blends, the samples were fractured under cryogenic conditions using liquid nitrogen. The fractured surfaces so obtained were immersed in tetrahydrofuran at room temperature for 30 min. The HTPB phases could be preferentially etched by the solvent while epoxy matrix phase remains unaffected. The etched specimens were dried to remove the solvents. The fracture surfaces were coated with thin layers of gold of about 100 Å. All specimens were examined with a Hitachi S210 scanning electron microscope (SEM) at an activation voltage of 15 kV.

Transmission Electron Microscopy (TEM). Transmission electron microscopy (TEM) was performed on a JEOL JEM-2010 high-resolution transmission electron microscope at an acceleration voltage of 120 kV. The samples were trimmed using a microtome machine, and the section samples were stained with OsO_4 to increase the contrast. The stained specimen sections (ca. 70 nm in thickness) were placed in 200 mesh copper grids for observations.

Atomic Force Microscopy (AFM). The AFM experiments were performed with a Nanoscope IIIa scanning probe microscope (Digital Instruments, Santa Barbara, CA). Tapping mode was employed in air using a tip fabricated from silicon (125 μm in length with ca. 300 kHz resonant frequency). Typical scan speeds during recording were 0.3–1 lines s^{-1} using scan heads with a maximum range of 16 \times 16 μm .

Results and Discussion

Synthesis and Characterization of PCL-PB-PCL. It has been reported that polybutadiene-*b*-poly(ϵ -caprolactone) (PB-

PCL) block copolymers can be synthesized by successive anionic polymerization.⁹ In the present work, the PCL-PB-PCL triblock amphiphilic copolymer was synthesized by the ring-opening polymerization of ϵ -CL, and a hydroxyl-terminated polybutadiene (HTPB) was used as the initiator and stannous octanoate [$\text{Sn}(\text{Oct})_2$] as the catalyst (Scheme 1). In the FTIR spectrum of the PCL-PB-PCL triblock copolymer, the ester carbonyls ($\text{C}=\text{O}$) of PCL are characteristic of the stretching vibration at ca. 1726 cm^{-1} ; the absorption bands at ca. 2943 cm^{-1} indicate the presence of methylene ($-\text{CH}_2-$) moieties in PCL subchains. The bands at 967 and 730 cm^{-1} are ascribed to *trans*-1,4 and *cis*-1,4 moieties in PB blocks, respectively; the weak absorption at 911 cm^{-1} is attributed to the 1,2-structures in the PB subchains. The FTIR results indicate that the as-synthesized polymer combined the structural feature of PCL and PB, which was further confirmed by nuclear magnetic resonance spectroscopy (NMR). From the ratio of the integration intensities of PB to those of PCL protons in the ^1H NMR spectrum, the molecular weight of the triblock copolymer was calculated to be $M = 14\,600$, which is in good agreement with the theoretical value, and thus the weight fraction of PB subchains in the block copolymer is 35%.

Miscibility and Phase Behavior of Binary Thermosetting Blends. To investigate the morphologies of epoxy blends with PCL-PB-PCL, it is mandatory to know the miscibility of binary blends of epoxy with PCL (and/or PB) (viz. the subchains of the triblock copolymer) after and before curing. Before curing, the binary blends comprised of DGEBA and PCL are miscible as rehearsed previously by us and other investigators;^{2c-g} the miscibility (or solubility) was ascribed to the negligible entropic contribution of mixing (ΔS_m) to free energy of mixing (ΔG_m) since the molecular weights of system are quite low. Upon adding MOCA (viz. the curing agent) to the binary DGEBA/PCL blends and curing at elevated temperatures, the epoxy thermosetting blends with PCL were obtained. The cured blends displayed single, composition-dependent glass transition temperatures (T_g) in the entire composition as revealed by means of differential scanning calorimetry (DSC),⁷ indicating that the cured blends are also miscible. The driving force for the miscibility has been ascribed to the formation of the intermolecular hydrogen bonding interactions⁷ between the aromatic amine-cross-linked epoxy and PCL. The miscibility of the binary blends composed of epoxy and the hydroxyl-terminated polybutadiene (HTPB) after and before curing were investigated in this work. Before curing, the binary mixtures composed of

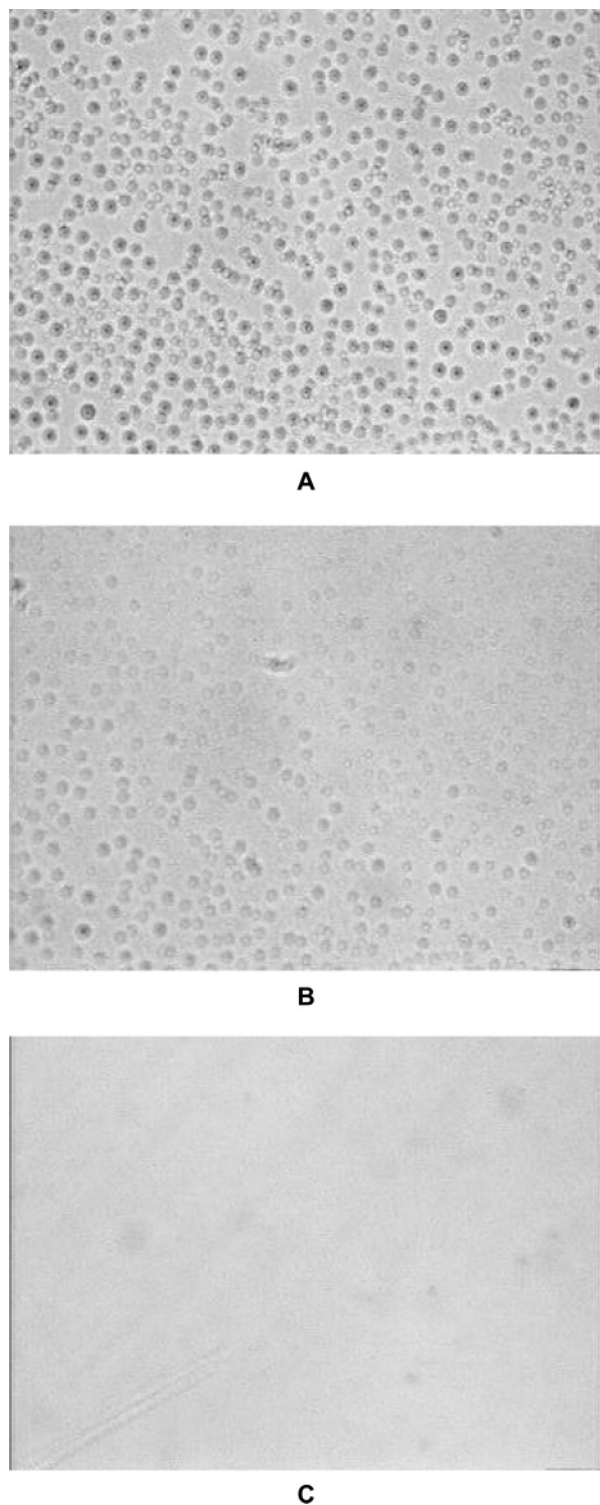


Figure 1. PCM micrographs of DGEBA/HTPB blends at (A) 100, (B) 120, and (C) 130 °C.

HTPB and the epoxy monomer (i.e., DGEBA) were cloudy at room temperature; however, the mixtures were transparent at elevated temperatures. This observation indicates that the blend system possesses an upper critical solution temperature (UCST) behavior; i.e., the increase in temperature leads to an increase in the miscibility. The cloud point curve of the system was measured by means of phase contrast microscopy (PCM) at a heating rate of 5 °C/min. The morphological evolution of the 70/30 DGEBA/HTPB blend as a function of temperature is shown in Figure 1. It is seen that at 100 °C the blend was heterogeneous (Figure 1A). With increasing the temperature,

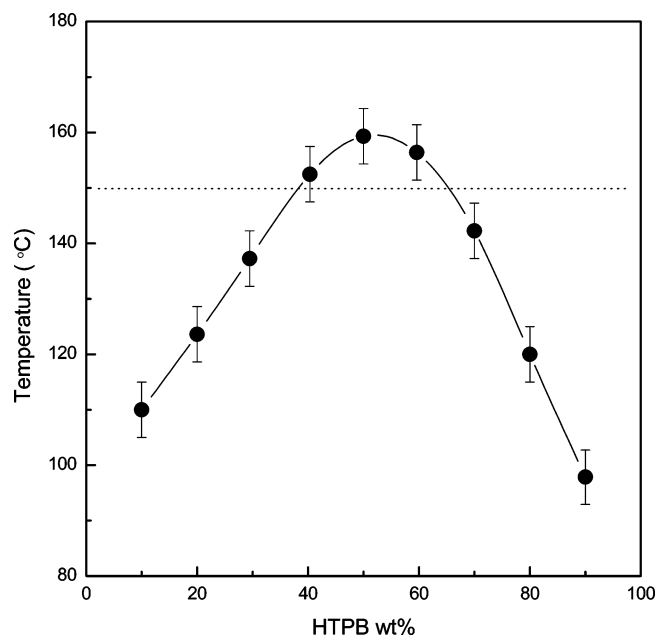


Figure 2. Cloud point curve of DGEBA/HTPB Blends. The dash line indicates the curing temperature.

the sample gradually became homogeneous (Figure 1B), and the homogeneous morphology was observed when the temperature was attained to 130 °C (Figure 1C). On the basis of the optical microscopic observation, the cloud point curve was obtained and is shown in Figure 2. It is seen that the phase boundary diagram is quite symmetrical with the upper critical solution temperature of 160 °C for the blend containing 50 wt % of HTPB. It is of interest to note that the maximum of the cloud point curve is different from that obtained for the mixture composed of DGEBA and carboxyl-terminated PB, reported by Verch et al.¹⁰ The difference could be due to the self-association of HTPB through the terminal hydroxyl groups.

The fact that miscibility of the mixtures was carried out at the elevated temperatures suggests that the curing reaction can be initiated from the homogeneous solutions when the curing temperatures are above the UCST of the system. Upon adding MOCA (i.e., the curing agent) to the system, the homogeneous and transparent ternary mixtures composed of DGEBA, MOCA, and PB were obtained while the temperature was increased up to 150 °C to initiate the curing reaction. With the curing reaction proceeding, the initial transparent solutions gradually became cloudy. This observation indicates that reaction-induced phase separation occurred during the curing. Figure 3 presents the SEM micrograph of THF-etched fracture surfaces of the curing blend containing 10 wt % HTPB. It is seen that the spherical particles (2.0 μm in diameter) were uniformly dispersed in the continuous epoxy matrix after HTPB phase was rinsed by THF. The spherical phase was attributed to HTPB, whereas the continuous phase was ascribed to the thermosetting matrix. This is a typical morphology of reaction-induced phase separation.

Formation of Nanostructures in Epoxy Thermosets Containing PCL–PB–PCL. *Protocol of Curing.* Before curing, the DGEBA/PCL–PB–PCL mixtures were transparent at 80 °C, suggesting the homogeneity of the mixtures in the molten state; i.e., no macroscopic phase separation occurred at the scale exceeding the wavelength of visible light. It should be pointed out that this clarity unnecessarily precludes the presence of the self-organized structures at the nanoscale at room temperature. In terms of the difference in miscibility of epoxy monomers with PCL and PB, it is proposed that the precursors of epoxy

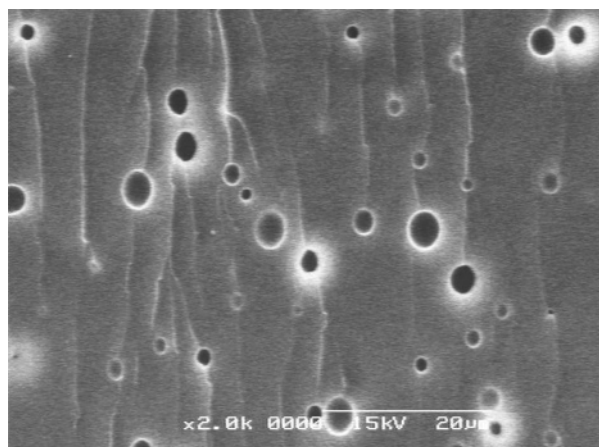
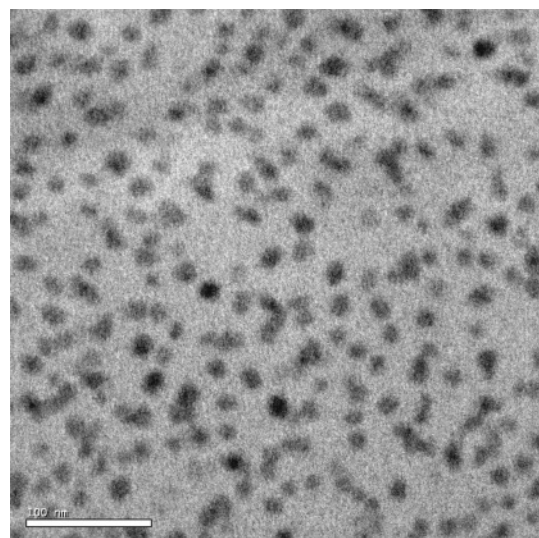


Figure 3. SEM micrograph of epoxy/HTPB 90/10 blends cured with MOCA.

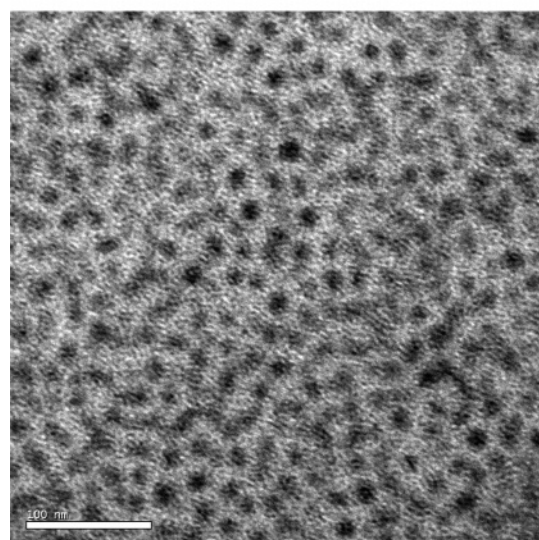
(i.e., the mixture of DGEBA and MOCA) are both the selective solvents for PCL blocks and nonsolvents for PB blocks at the lower temperature. In this work, the contents of PCL-PB-PCL in thermosets were controlled up to 50 wt %, which correspond to the concentration of PB up to 17.5 wt % in the thermosets. The curing temperature was set as 150 °C, which is much higher than the corresponding upper critical solution temperatures (UCST), to ensure that the curing reactions were carried out without the presence of self-assembly structures. Therefore, the formation of the nanostructures (if any) in the thermosets should not result from the self-organized structures formed before curing.

Formation of Nanostructures. All the epoxy thermosets containing PCL-PB-PCL were transparent above the melting point of PCL (e.g., 80 °C), indicating that no macroscopic phase separation occurred at least on the scale exceeding the wavelength of visible light. The morphologies of the thermosets were investigated by transmission electronic microscopy (TEM), small-angle X-ray scattering (SAXS), and atomic force microscopy (AFM). The TEM micrographs of the thermosets containing 10, 20, and 30 wt % of the triblock copolymer are presented in Figure 4. The heterogeneous morphology at the nanoscopic level was found in all the cases. The dark objects are assigned to PB microphases since the PB domains containing C=C double bonds were preferentially stained with O_3O_4 whereas epoxy matrix and PCL were almost unaffected. For the thermoset containing 10 wt % of PCL-PB-PCL, the spherical PB domains were dispersed in the continuous epoxy matrix with an average size of ca. 10 nm (Figure 4A). The number of the spherical objects increased whereas the average distance between adjacent domains decreased with increasing the content of PCL-PB-PCL in the thermosets. It is seen that the size of the nanoparticles almost remains invariant (see Figure 4B). It is noted that when the content of PCL-PB-PCL is 20 wt %, the spherical particles began to interconnect to some extent (Figure 4B). Therefore, the thermoset at this composition possesses a combined morphology, in which both spherical PB domains and some interconnected PB domains were simultaneously present. When the content of PCL-PB-PCL was increased up to 30 wt %, the domains of PB were highly interconnected, forming interconnected objects at the nanometer scales. This morphology is a typical structure of bicontinuous microphase separation.

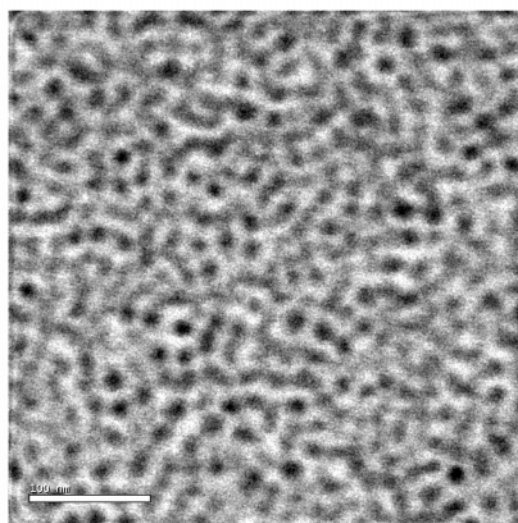
Shown in Figure 5 are the SAXS profiles of the thermosets containing 10, 20, and 30 wt % of the triblock copolymer. The well-defined scattering peaks were observed in all the cases, indicating that the thermosets are microphase-separated. Ac-



A



B



C

Figure 4. TEM micrographs of epoxy/PCL-PB-PCL blends cured with MOCA containing (A) 10, (B) 20, and (C) 30 wt % of PCL-PB-PCL. The scale bar equals 100 nm.

cording to the position of the primary scattering peaks, the average distance ($L = 2\pi/q_m$) between neighboring domains

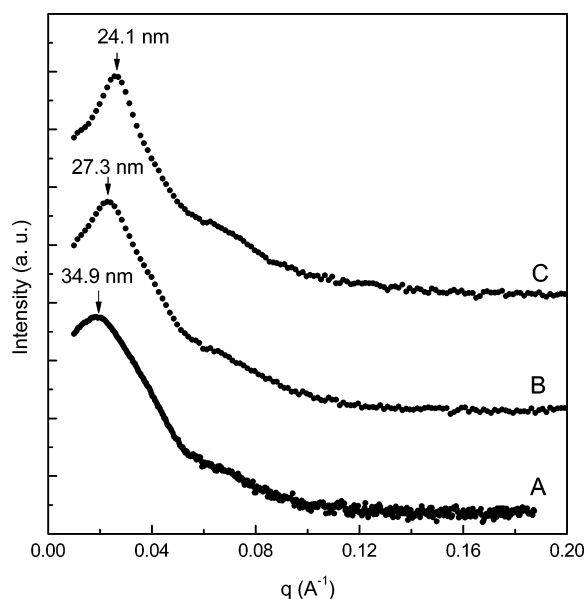


Figure 5. SAXS profiles epoxy/PCL-PB-PCL blends cured with MOCA containing (A) 10, (B) 20, and (C) 30 wt % of PCL-PB-PCL.

can be estimated to be 34.9, 27.3, and 24.1 nm for the thermosets containing the block copolymer of 10, 20, and 30 wt %, respectively. It is seen that the average distance between neighboring domains decreased with increasing the content of the triblock copolymer. These results are in a good agreement with those obtained by means of TEM.

The morphologies of the nanostructured epoxy thermosets were further observed by means of AFM. The AFM images of the thermosets containing 10, 20, 30, and 40 wt % of the triblock copolymer are presented in Figure 6. The left and right are the topography and phase images, respectively. The light (or gray) continuous regions are ascribed to the epoxy-rich components composed of the cross-linked epoxy networks which were interpenetrated by the PCL blocks of the copolymer whereas the dark areas correspond to PB domains. For the thermoset containing 10 wt % of PCL-PB-PCL, the nanosized separate particles were imbedded in the continuous epoxy matrix at the average size of ca. 10–20 nm in diameter (Figure 6A). With increasing the content of the block copolymer, the nanosized separate PB particles began to coagulate in the continuous epoxy matrix, and some wormlike objects of PB appeared (Figure 6B). When the concentration of PCL-PB-PCL was more than 30 wt %, the epoxy component began to form some separated nanosized particles or wormlike objects (Figure 6C,D). It should be pointed out that the micrographs of AFM are a little different from those obtained with TEM since the two techniques detect the information on phase behavior from different side views of structure. The former are obtained on the basis of the difference in transmitted electronic densities through samples whereas the latter reflects the information about tip-sample interactions resulting from adhesion,^{11a} surface stiffness,^{11b} and viscoelastic effects.^{11c–e} Therefore, the AFM results could be more sensitive to the transition region between PB domain and the epoxy matrices that were interpenetrated by PCL chains. Nonetheless, the AFM experiments indeed indicate that the nanostructured epoxy thermosets were obtained.

Interpretation of Nanostructures. The formation of nanostructures in this work was realized by controlling the microphase separation of PB blocks induced by reaction, other than by fixing the preformed self-assembly microphases in the mixtures of the block copolymer and the epoxy precursors. The

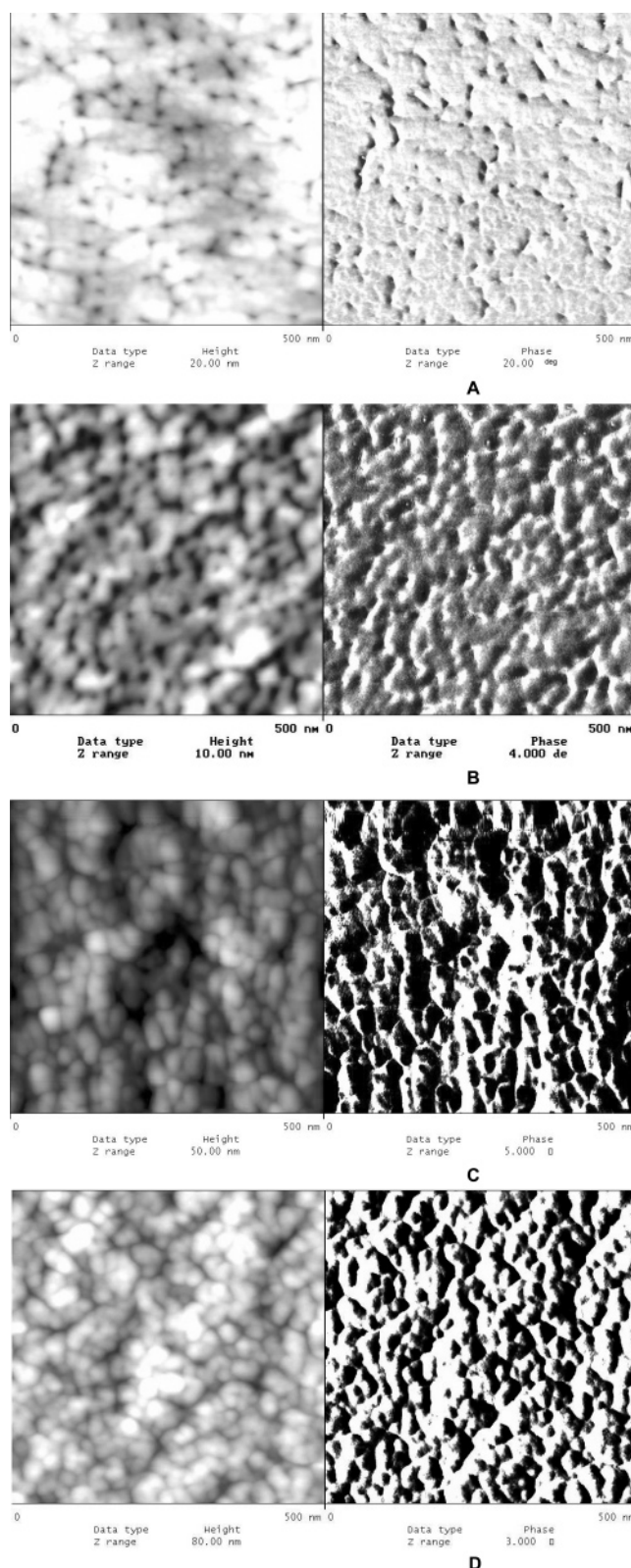


Figure 6. AFM images of the thermosets containing (A) 10, (B) 20, (C) 30, and (D) 40 wt % of PCL-PB-PCL. Left: topography; right: phase contrast.

driving force for the reaction-induced microphase separation of PB blocks is the decrease in entropic contribution to free energy of mixing for the mixing of PB blocks with cross-linked epoxy networks. Nonetheless, the PCL blocks are miscible with the cross-linked epoxy networks; i.e., the subchains of PCL were interpenetrated into the cross-linked epoxy network at the segmental level. To confirm the above speculation, the phase

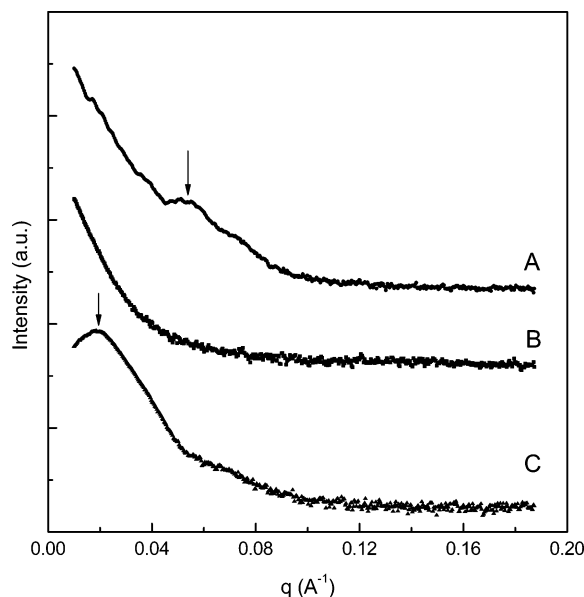


Figure 7. SAXS profiles epoxy blends cured with MOCA containing 10 wt % PCL-PB-PCL: (A) the mixture of DGEBA, DDM, and PCL-PB-PCL at 25 °C; (B) the mixture at the beginning of cure at 150 °C; (C) the blends after cured at 150 °C for 4 h.

behavior of the blends of epoxy precursors with triblock copolymer was examined by SAXS prior to cure and after each stage of cure. Figure 7 representatively presents the SAXS profiles of the blend containing 10 wt % of PCL-PB-PCL. At room temperature, the blend shows a peak at $q = 0.05 \text{ \AA}^{-1}$, corresponding a long period of 11.6 nm (see curve A). This observation indicates that the ternary mixture of PCL-PB-PCL, DGEBA, and DDM possesses microphase-separated structure at room temperature. It is proposed that the micelle structure is formed in the mixture since the precursors of epoxy (viz. the mixture of DGEBA and DDM) behave as the selective solvent of the triblock copolymer. It was noted that when the system was heated to 80 °C or higher, the scattering peak began to disappear, suggesting that the micelle structure was destroyed at elevated temperature. This result is identical with the UCST phase behavior of DGEBA and HTPB blends. The fact that no reflection peak was found for the blend upon heating to 150 °C indicates that the system is homogeneous at the beginning of curing reaction (see curve B). With the curing proceeding at 150 °C, the microphase-separated structure reappeared as shown by the presence of the well-defined scattering peak (see curve C). It is worth noticing that the long period of the thermosetting sample (ca. 31.4 nm) is quite higher than that of the blend prior to cure (ca. 11.6 nm). This observation could be explained on the basis of the effect of curing reaction on the morphology. Prior to cure, the domain of PB could be swollen by the precursors of epoxy and thus the smaller distances between adjacent PB domains were observed. Upon curing at elevated temperature, the PB domains were via reaction-induced microphase separation, which will no longer be swollen by the precursors of epoxy. Therefore, the average distances between the neighboring spherical domains were increased. The SAXS results indicate that at the curing temperature the curing reaction was indeed started from the homogeneous solutions comprised of the epoxy precursors and PCL-PB-PCL.

To ascertain the mixing degree of the cross-linked epoxy networks with PCL, differential scanning calorimetry (DSC) and Fourier transform infrared spectroscopy (FTIR) were employed. Shown in Figure 8 are the DSC thermographs of the nanostructured epoxy thermosets. The DSC curve of PCL-PB-PCL

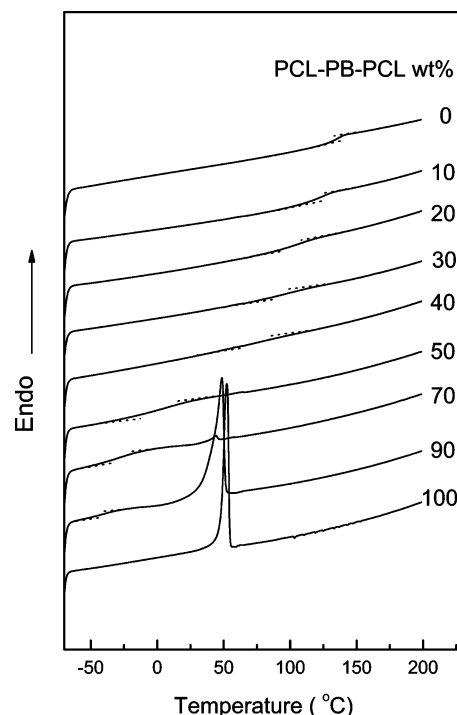


Figure 8. DSC curves of the nanostructured epoxy thermosets.

triblock copolymer displayed a sharp endothermic peak at 52 °C, which is ascribed to the melting transition of PCL subchains. It is noted that all the thermosets with the concentration of triblock copolymer less than 50 wt % did not exhibit the melting transition, suggesting that the PCL blocks in these nanostructured thermosets are not crystalline. It is plausible to propose that the PCL blocks were interpenetrated in the cross-linked epoxy networks; i.e., the PCL blocks are miscible with the epoxy networks. The behavior of miscibility was further confirmed by the changes in glass transition temperatures (T_g 's). It should be pointed out that the glass transition temperatures indicated in the DSC curves should be ascribed to the cross-linked epoxy networks. From Figure 9, it is seen that the major T_g 's of the nanostructured thermosets significantly depressed upon adding PCL-PB-PCL to the systems. The T_g 's increasingly shifted to lower temperatures with increasing the content of block copolymer (Figure 9). This case is in a good agreement with miscible binary thermosetting blend of epoxy with PCL.⁷ In addition, it is worth noticing that the widths of the glass transition region for the nanostructured thermosets are significantly higher than that of the control epoxy. The broadening of the glass transition range could be attributed to the enrichment of soft PCL chains around the PB microphases; i.e., only the cross-linked epoxy matrices near the front of PB domains were efficiently plasticized by PCL chains and exhibited the lower glass transition temperatures (T_g 's) than the epoxy matrices that was not interpenetrated by PCL blocks.

The evidence that the cross-linked epoxy networks near the front of PB domains were interpenetrated by PCL blocks can be obtained from the results of Fourier transform infrared spectroscopy (FTIR). Shown in Figure 10 are the FTIR spectra of PCL-PB-PCL and the nanostructured thermosets in the range of 1600–1800 cm^{-1} . The absorption bands are ascribed to the stretching vibration of carbonyl groups (C=O) in PCL blocks. At the room temperature, the carbonyl band of the PCL-PB-PCL triblock copolymers consists of two components sensitive to the conformation of PCL chains. The one component centered at 1735 cm^{-1} is characteristic of amorphous chains of

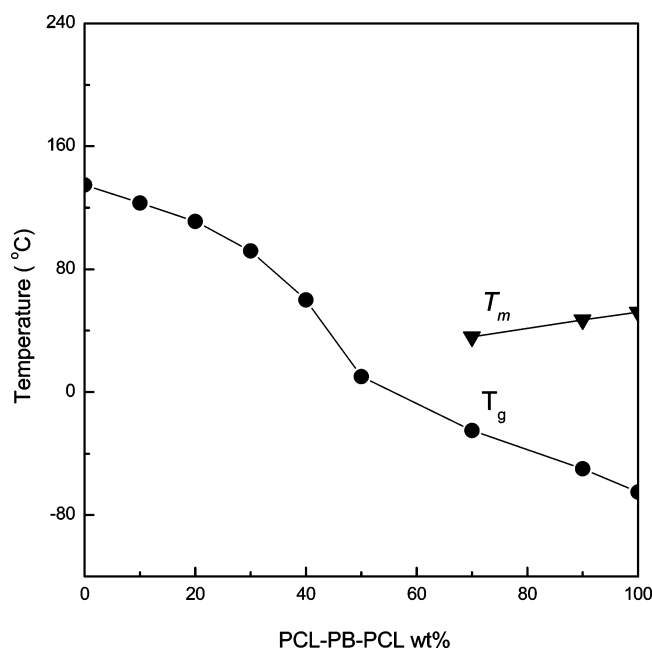


Figure 9. Plot of glass transition temperatures (T_g 's) as a function of PCL-PB-PCL content.

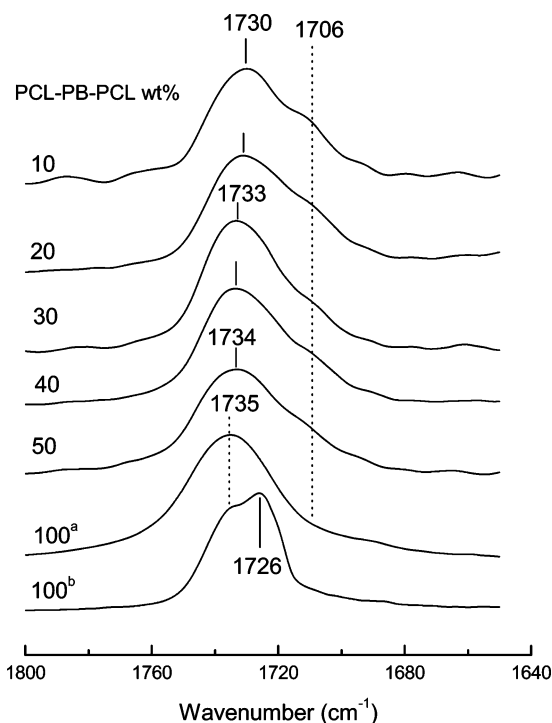
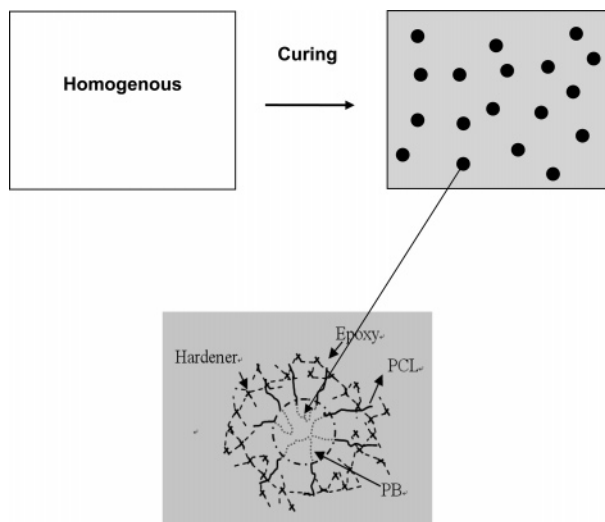


Figure 10. FTIR spectra of the nanostructured thermosets in the range of 1600–1800 cm^{-1} : (a) at 80 °C; (b) at 25 °C.

PCL whereas the sharp band at 1726 cm^{-1} is ascribed to the carbonyls in the crystalline region of PCL. Upon heating the block copolymer up to 80 °C, the band at 1726 cm^{-1} disappeared, indicating the fusion of PCL crystals. In the nanostructured thermosets, the bands of the PCL crystals were absent, implying that PCL blocks exist in the thermosets in the amorphous state. Nonetheless, there appeared new shoulders at the lower frequency of 1706 cm^{-1} in all the nanostructured thermosets. The shoulder bands could be ascribed to the stretching vibration of the hydrogen-bonded carbonyls. In the meantime, the band at 1735 cm^{-1} was seen to shift to the lower frequency (1730 cm^{-1}). The FTIR results demonstrate that the intermolecular hydrogen-bonding interactions between the car-

Scheme 2. Preparation of Nanostructured Epoxy Thermosets



bonyls of PCL and the hydroxyl groups of cross-linked epoxy networks were formed in the nanostructured thermosets; i.e., PCL blocks are miscible with the epoxy matrices, which is in accordance with the results of thermal analysis. It is proposed that the formation of the intermolecular specific interactions between the cross-linked epoxy networks and PCL subchains is a decisive factor to suppress the microphase separation of PCL blocks due to the decrease in entropic contribution resulting from the polymerization.

In terms of the above results, the structural evolution in the thermosetting system is proposed and is illustrated in Scheme 2. At the lower temperature, the self-organized microphase (viz. PB domains) exists in the mixture of the precursors (DGEBA and MOCA) of epoxy and PCL-PB-PCL. However, the elevated temperatures destroyed the self-organized structure. In this work, the curing temperature was set as 150 °C, which is much higher than the UCST, and thus the curing reaction was initiated from the homogeneous solution. With the curing reaction proceeding, the PB blocks were separated out whereas the PCL blocks remained in the cross-linked epoxy networks. The microphase separation of PB block was driven by the increased molecular weight of system due to polymerization. It should be pointed out that the demixing of PB subchains could be taken as a kind of confined microphase separation induced by polymerization since one end of PB subchain was constricted by the miscible PCL subchain. The mixing of PCL blocks with the cross-linked epoxy networks could be ascribed to the formation of the intermolecular specific interactions between the two components. It is proposed that the rubbery midlocks (viz. PB) could take the conformation of loops or bridges¹² since both the end blocks (viz. PCL) were physically tethered into the epoxy matrices. It should be pointed out that the reaction-induced microphase separation could be different from the cases of macroscopic phase separation induced by polymerization in the mixtures of a homopolymer (or random copolymer) and monomers of thermosets, and the investigation of the kinetics could be an interesting subject.

Conclusions

The amphiphilic triblock copolymer poly(ϵ -caprolactone)-*b*-polybutadiene-*b*-poly(ϵ -caprolactone) (PCL-PB-PCL) was synthesized via the ring-opening polymerization of ϵ -caprolactone in the presence of a hydroxyl-terminated polybutadiene (HTPB), which was catalyzed by stannous octanoate [$\text{Sn}(\text{Oct})_2$].

The amphiphilic triblock copolymer was further used to prepare nanostructured epoxy thermosets. The in situ polymerization of epoxy monomers in the presence of PCL–PB–PCL started from the homogeneous solution composed of the block copolymer and the monomers of epoxy at the temperature above the upper critical solution temperature (UCST) of diglycidyl ether of bisphenol A (DGEBA) and HTPB. The results of transmission electron microscopy (TEM), small-angle X-ray scattering (SAXS), and atomic force microscopy (AFM) showed that the nanostructured thermosets were successfully obtained. The formation of the nanostructures was judged to be via polymerization-induced microphase separation of PB subchains of PCL–PB–PCL triblock copolymers whereas the PCL subchains remained mixed with the cross-linked epoxy networks. The miscibility can be accounted for the T_g depression of epoxy matrix and the intermolecular specific interactions between cross-linked epoxy and PCL. The formation mechanism of the nanostructure is in a marked contrast to the strategy in which some equilibrium self-organized structures were preformed and the microphases were fixed via subsequent curing reaction.

Acknowledgment. The financial support from Natural Science Foundation of China (Project No. 20474038 and 50390090) is acknowledged. S.Z. thanks Shanghai Educational Development Foundation, China, under an Award (2004-SG-18) to “Shuguang Scholar”.

References and Notes

- (1) (a) Pascault, J. P.; Williams, R. J. J. In *Polymer Blends*; Paul, D. R., Bucknall, C. B., Eds.; Wiley: New York, 2000; Vol. 1, pp 379–415. (b) Guo, Q. In *Polymer Blends and Alloys*; Shonai, G. O., Simon, G., Eds.; Marcel Dekker: New York, 1999; Chapter 6, pp 155–187.
- (2) (a) Luo, X.; Zheng, S.; Zhang, N.; Ma, D. *Polymer* **1994**, *35*, 2619. (b) Zheng, S.; Zhang, N.; Luo, X.; Ma, D. *Polymer* **1995**, *36*, 3609. (c) Guo, Q.; Harrats, C.; Groeninckx, G.; Reynaers, H.; Koch, M. H. J. *Polymer* **2001**, *42*, 6031. (d) Guo, Q.; Groeninckx, G. *Polymer* **2001**, *42*, 8647. (e) Zheng, S.; Zheng, H.; Guo, Q. *J. Polym. Sci., Part B: Polym. Phys.* **2003**, *41*, 1085. (f) Zheng, S.; Guo, Q.; Chan, C.-M. *J. Polym. Sci., Part B: Polym. Phys.* **2003**, *41*, 1099. (g) Chen, J.-L.; Chang, F.-C. *Macromolecules* **1999**, *32*, 5348. (h) Zheng, H.; Zheng, S.; Guo, Q. *J. Polym. Sci., Part A: Polym. Chem.* **1997**, *35*, 3161. (i) Zheng, H.; Zheng, S.; Guo, Q. *J. Polym. Sci., Part A: Polym. Chem.* **1997**, *35*, 3169. (j) Mucha, M. *Colloid Polym. Sci.* **1994**, *272*, 1090.
- (3) (a) Hillmyer, M. A.; Lipic, P. M.; Hajduk, D. A.; Almdal, K.; Bates, F. S. *J. Am. Chem. Soc.* **1997**, *119*, 2749. (b) Lipic, P. M.; Bates, F. S.; Hillmyer, M. A. *J. Am. Chem. Soc.* **1998**, *120*, 8963.
- (4) (a) Mijovic, J.; Shen, M.; Sy, J. W.; Mondragon, I. *Macromolecules* **2000**, *33*, 5235. (b) Guo, Q.; Thomann, R.; Gronski, W. *Macromolecules* **2002**, *35*, 3133. (c) Guo, Q.; Thomann, R.; Gronski, W. *Macromolecules* **2003**, *36*, 3635. (d) Ritzenthaler, S.; Court, F.; Girard-Reydet, E.; Leibler, L.; Pascault, J. P. *Macromolecules* **2002**, *35*, 6245. (e) Ritzenthaler, S.; Court, F.; Girard-Reydet, E.; Leibler, L.; Pascault, J. P. *Macromolecules* **2003**, *36*, 118. (f) Kosonen, H.; Ruokolainen, J.; Nyholm, P.; Ikkala, O. *Macromolecules* **2001**, *34*, 3046. (g) Kosonen, H.; Ruokolainen, J.; Nyholm, P.; Ikkala, O. *Polymer* **2001**, *42*, 9481. (h) Kosonen, H.; Ruokolainen, J.; Torkkeli, M.; Serimaa, R.; Nyholm, P.; Ikkala, O. *Macromol. Chem. Phys.* **2002**, *203*, 388. (i) Grubbs, R. B.; Dean, J. M.; Broz, M. E.; Bates, F. S. *Macromolecules* **2000**, *33*, 9522. (k) Rebizant, V.; Abetz, V.; Tournihac, T.; Court, F.; Leibler, L. *Macromolecules* **2003**, *36*, 9889. (l) Dean, J. M.; Verghese, N. E.; Pham, H. Q.; Bates, F. S. *Macromolecules* **2003**, *36*, 9267. (m) Rebizant, V.; Venet, A. S.; Tournihac, F.; Girard-Reydet, E.; Navarro, C.; Pascault, J. P.; Leibler, L. *Macromolecules* **2004**, *37*, 8017. (n) Dean, J. M.; Grubbs, R. B.; Saad, W.; Cook, R. F.; Bates, F. S. *J. Polym. Sci., Part B: Polym. Phys.* **2003**, *41*, 2444. (o) Wu, J.; Thio, Y. S.; Bates, F. S. *J. Polym. Sci., Part B: Polym. Phys.* **2005**, *43*, 1950. (p) Guo, Q.; Dean, J. M.; Grubbs, R. B.; Bates, F. S. *J. Polym. Sci., Part B: Polym. Phys.* **2003**, *41*, 1994.
- (5) Flory, P. J. *Principles of Polymer Chemistry*; Cornell University Press: Ithaca, NY, 1953.
- (6) (a) Buchholz, U.; Mülhaupt, R. *ACS Polym. Prepr.* **1992**, *33*, 205. (b) Könczöl, L.; Döll, W.; Buchholz, U.; Mülhaupt, R. *J. Appl. Polym. Sci.* **1994**, *54*, 815. (c) Serrano, E.; Martin, M. D.; Tercjak, A.; Pomposo, J. A.; Mecerreyes, D.; Mondragon, I. *Macromol. Rapid Commun.* **2005**, *26*, 982.
- (7) (a) Yin, M.; Zheng, S. *Macromol. Chem. Phys.* **2005**, *206*, 929. (b) Ni, Y.; Zheng, S. *Polymer* **2005**, *46*, 5828.
- (8) Tanaka, H.; Nishii, T. *Phys. Rev. A* **1989**, *39*, 783.
- (9) (a) Nojima, S.; Wang, D.; Ashida, T. *Polym. J.* **1991**, *23*, 1473. (b) Nojima, S.; Kato, S.; Yamamoto, S.; Ashida, T. *Macromolecules* **1992**, *25*, 2237. (c) Nojima, S.; Nakano, H.; Takahashi, Y.; Ashida, T. *Polymer* **1994**, *35*, 3479. (d) Hsieh, H. L.; Quirk, R. P. *Anionic Polymerization, Principles and Practical Applications*; Marcel Dekker: New York, 1996. (e) Rozenberg, B. A.; Estrin, Y. I.; Estrina, G. A. *Macromol. Symp.* **2000**, *153*, 197.
- (10) Verchere, D.; Sautereau, H.; Pascault, J. P.; Moschiar, S. M.; Riccardi, C. C.; Williams, R. J. J. *Polymer* **1989**, *30*, 107.
- (11) (a) Schmitz, I.; Schreiner, M.; Friedbacher, G.; Grasserbauer, M. *Appl. Surf. Sci.* **1997**, *115*, 190. (b) Magonov, S. N.; Elings, V.; Whangbo, M. H. *Surf. Sci.* **1997**, *375*, L385. (c) Tamayo, A.; Garcia, R. *Langmuir* **1996**, *12*, 4434. (d) Chen, X.; McGurk, S. L.; Davies, M. C.; Roberts, C. J.; Shakesheff, K. M.; Davies, J.; Dawkes, D. A. *Macromolecules* **1998**, *31*, 2278. (e) Clarke, S.; Davies, M. C.; Roberts, C. J.; Tendler, S. J. B.; Williams, P. M.; Lewis, A. L.; O'Bryne, V. *Macromolecules* **2001**, *34*, 4166.
- (12) (a) Watanabe, H.; Sato, T.; Osaki, K.; Yao, M. L.; Yamagishi, A. *Macromolecules* **1997**, *30*, 5877. (b) Watanabe, H.; Sato, T.; Osaki, K. *Macromolecules* **2000**, *33*, 1686. (c) Watanabe, H.; Sato, T.; Osaki, K. *Macromolecules* **2000**, *33*, 2545.

MA0518499